

# Buckling behavior of strengthened perforated plates under shear loading

Bin Cheng\* and Chun Li

*Department of Civil Engineering, Shanghai Jiao Tong University, Shanghai, China*

*(Received February 03, 2012, Revised July 18, 2012, Accepted July 24, 2012)*

**Abstract.** This paper is dedicated to the buckling behaviors of strengthened perforated plates under edge shear loading, which is a typical load pattern of steel plates in civil engineering, especially in plate and box girders. The square plates considered each has a centric circular hole and is simply supported on four edges in the out-of-plane direction. Three types of strengthening stiffeners named ringed stiffener (*RS*), flat stiffener (*FSA* and *FSB*) and strip stiffener (*SSA*, *SSB* and *SSC*) are mainly discussed. The finite element method (FEM) has been employed to analyse the elastic and elasto-plastic buckling behavior of unstrengthened and strengthened perforated plates. Results show that most of the strengthened perforated plates behave higher buckling strengths than the unstrengthened ones, while the enhancements in elastic buckling stress and elasto-plastic ultimate strength are closely related to stiffener types as well as plate geometric parameters including plate slenderness ratio and hole diameter to plate width ratio. The critical slenderness ratios of shear loaded strengthened perforated plates, which determine the practical buckling pattern (i.e., elastic or elasto-plastic buckling) of the plates, are also studied. Based on the contrastive analyses of strengthening efficiency considering the influence of stiffener consumption, the most efficient cutout-strengthening methods for shear loaded perforated square plates with different slenderness ratios and circular hole diameter to plate width ratios are preliminarily identified.

**Keywords:** strengthened perforated plate; circular hole; shear loading; elastic buckling stress; elasto-plastic ultimate strength; cutout-strengthening.

---

## 1. Introduction

Perforations are often provided in steel structures such as plate and box girders, box pylons and ship grillages for the purposes of access, services even aesthetics. The mechanical behaviors of plates containing holes are different from those of unperforated plates. As reported in existing literatures, decreases in elastic buckling stress and elasto-plastic ultimate strength, when compared to unperforated plate, are often observed in perforated plates. When the cutout is unavoidable for the plate under high working stress, the reduced buckling strength of the perforated plate may be unable to meet the requirement of normal serviceability or structural safety. Hence, it is necessary to adopt an appropriate cutout-strengthening method to improve the buckling behaviors of perforated plates in these situations.

Plenty of studies about the buckling behavior of perforated plates have been undertaken and the load cases of uniaxial and biaxial compression have been focused by Narayanan and Rockey (1981),

---

\* Corresponding author, Associate Professor, E-mail: [cheng\\_bin@sjtu.edu.cn](mailto:cheng_bin@sjtu.edu.cn)

Shanmugam and Narayanan (1982), Azizian and Roberts (1983), Narayanan and Chow (1984), Brown (1990), Shanmugam *et al.* (1999), El-Sawy, Nazmy and Martini (2001, 2004, 2007, 2010), Paik (2007), Moen and Schafer (2009), Wang *et al.* (2009), Komur (2011), and Maiorana *et al.* (2011), with conclusions, suggestions and formulations about the elastic and elasto-plastic buckling behaviors of the perforated plates with various plate parameters (i.e., plate aspect ratio and plate slenderness ratio) and hole parameters (i.e., hole shape, hole size and hole location) having been presented. The elastic buckling coefficients of shear loaded square plates containing circular, square and rectangular holes are predicted by Sabir and Chow (1983), Brown and Yettram (1986), and Brown *et al.* (1987), respectively. Paik (2007, 2008) investigated the ultimate strength of perforated steel plates under edge shear loading and the combined biaxial compression and edge shear loads. Pellegrino *et al.* (2009) dedicated to the linear and non-linear behavior of shear loaded steel plates with circular and rectangular holes. Wang *et al.* (2009) also carried out finite element parametric analysis on buckling and ultimate strength of plate panels with openings under shear stress. However, there is few researcher (Cheng and Zhao 2010) concerning about the cutout-strengthening methods used for improving the degraded buckling behavior of perforated plates in the published literatures.

The aim of the present paper is to investigate the buckling behaviors of strengthened perforated steel plates under edge shear loading, which is a typical load pattern in building, bridge, and ship structures. The studied square plates with centric circular holes are considered to be simply supported on all edges. Three types of strengthening stiffeners, i.e., ringed stiffener (*RS*), flat stiffener (*FSA* and *FSB*) and strip stiffener (*SSA*, *SSB*, and *SSC*), are taken into account. A series of profound investigations of both elastic and elasto-plastic buckling behaviors for strengthened and unstrengthened perforated plates are carried out by the use of ANSYS finite element analysis programme, since the elastic buckling stress and elasto-plastic ultimate strength are useful for the serviceability limit state (SLS) and ultimate limit state (ULS) design purposes, respectively. Additionally, the most efficient cutout-strengthening methods for shear loaded perforated square plates with different slenderness ratios and circular hole diameter to plate width ratios are preliminarily identified on the basis of contrastive analyses of strengthening efficiency considering the influence of stiffener consumption.

## 2. Perforated square plates

### 2.1 Geometry

The perforated square plates, with a centric circular hole for each one, are employed as research objects in this paper, and the following two geometric parameters are considered:

- plate slenderness ratio  $b/t$ , varying from 20 to 100 with increment of 10,
- hole diameter to plate width ratio  $d/b$ , varying from 0.1 to 0.5 with increment of 0.1,

where  $b$  and  $t$  is the width and thickness of the square plate,  $d$  is the diameter of the circular hole, as shown in Fig. 1.

Three types of stiffeners named ringed stiffener (*RS*), flat stiffener (*FS*) and strip stiffener (*SS*) are considered in the present study due to the convenience in practical engineering. The flat stiffener and strip stiffener are redivided into two (i.e., *FSA* and *FSB*) and three (i.e., *SSA*, *SSB* and *SSC*) subcategories, respectively, according to the various orientations of the stiffener. The details of the strengthened perforated plates are shown in Fig. 2:

- (1) For the plates strengthened by ringed stiffeners (*RS*-plate), a strengthening stiffener with thickness

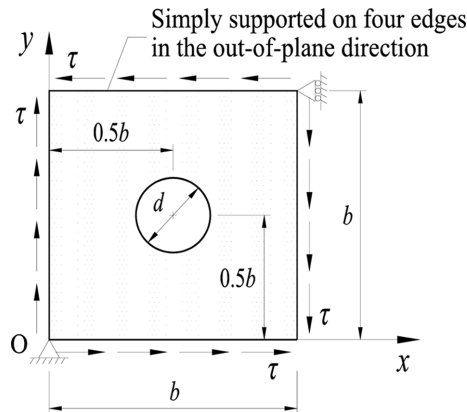


Fig. 1 The unstrengthened square plate with a centrally placed circular hole under edge shear loading

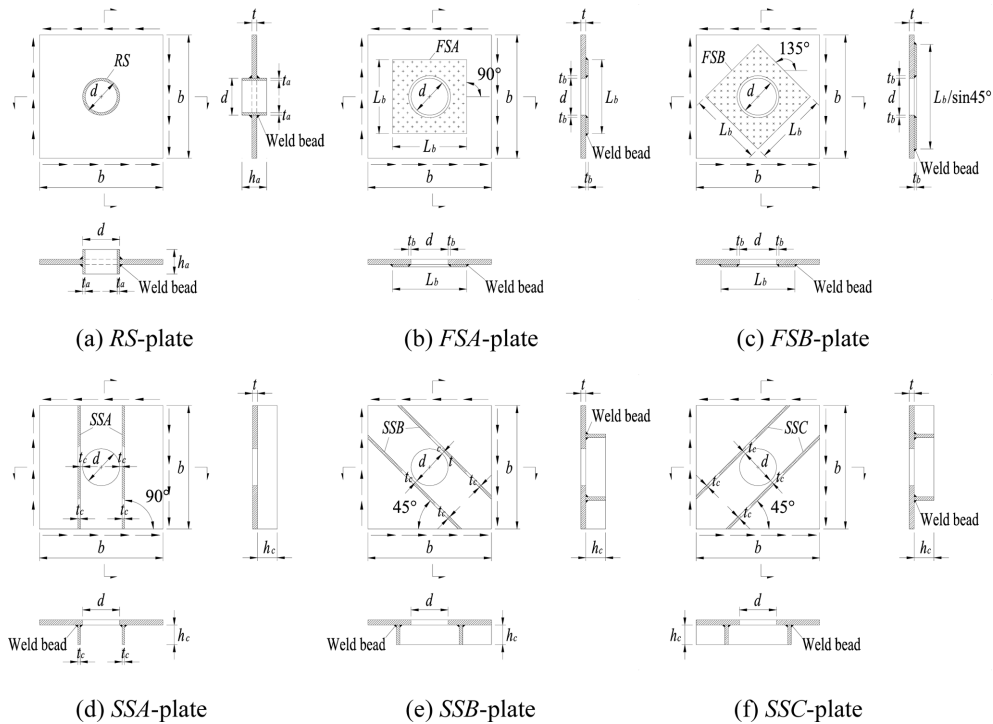


Fig. 2 The strengthened perforated square plate with a centric circular hole

of  $t_a$  and width of  $h_a$  is symmetrically welded to the perforated plate at their circular intersections after being rolled into a ring with outer diameter of  $d$ .

(2) For the plates strengthened by flat stiffeners (*FSA*-plate and *FSB*-plate), three fabricating steps are normally suggested. Firstly, a circular hole with diameter of  $(d + 2t_b)$ , where  $t_b$  is the thickness of square flat stiffener with width of  $L_b$ , should be perforated in center of the stiffener. The perforated stiffener, then, is tightly attached to the surface of the plate strengthened with two circles in the plate and the

stiffener being concentric. The welding is finally carried out along the inner (hole) edge and the four outer edges of the flat stiffener.

(3) For the plates strengthened by strip stiffeners (*SSA*-plate, *SSB*-plate and *SSC*-plate), the two stiffeners with thickness of  $t_c$  and width of  $h_c$  are parallel or skewed to the shear load direction after being welded to the perforated plate, and the smallest distance between hole edge and stiffener's surface, as used for welding, is selected as the same value of stiffener thickness.

Considering the common situations of practical engineering, the geometric sizes (interpreted in Fig. 2) of stiffeners selected in the following analyses take the values as:

- For ringed stiffener (*RS*),  $t_a = 0.5t$ ,  $h_a = 10t_a$ .
- For flat stiffener (*FSA* and *FSB*),  $t_b = 0.5t$ ,  $L_b = 1.8d$ .
- For strip stiffener (*SSA*, *SSB* and *SSC*),  $t_c = 0.5t$ ,  $h_c = 8t_c$ .

## 2.2 Boundary conditions

A perforated plate in practical structure is normally supported by the adjacent plates and thus is in the state between rotatable constraint and fixed constraint (i.e., partially restrained in rotation) in the out-of-plane direction. The studied plates, therefore, are considered to be simply supported on all edges in the present study, as shown in Fig. 1. It means that the lateral deflection stiffnesses on the boundaries are infinite and the rotational stiffnesses on the edges are infinitesimal.

Furthermore, some in-plane boundary conditions should be applied to the finite element model considering the nonoccurrence of rigid-body movement and the permission of translational displacement in the plate plane. In this paper, the left-bottom corner of the plate is restrained in the  $x$  and  $y$  directions and the degrees of freedom of the right-top corner are fixed in the  $x$  direction, as shown in Fig. 1.

## 2.3 Load case

In-plane loads including compression, tension and shear loading should be mainly considered according to the practical situations in engineering. In this study, only uniform shear loading which is one of the dominant load cases in plate and box girders, as shown in Fig. 1, is focused on.

## 3. Analysis method and FE model

### 3.1 Basic hypotheses

The study is based on the following assumptions:

1. The perforated plate and the stiffener are composed of the same isotropic material.
2. The load effect of steel weight is ignored.
3. The perforated plate and the stiffener are rigidly connected at their intersections.
4. The influences of weld bead size and welding induced residual stress are ignored.

### 3.2 Buckling analysis method

The governing equation for the finite element analysis can be written in incremental representation as follows

$$\Delta R = (K_0 + K_\sigma)\Delta u \quad (1)$$

where  $K_0$  is the constant stiffness matrix related only to the geometric sizes of the plate,  $K_\sigma$  is the current stress stiffness matrix,  $\Delta u$  is the incremental displacement vector,  $\Delta R$  is the corresponding incremental force vector.

When elastic buckling occurs, the plate behaves increase in its displacements  $\Delta u$  with no increase in the load or force  $\Delta R$ . It can be concluded from Eq. (1) that  $|K_0 + K_\sigma| = 0$  is satisfied. Taking advantage of the proportional relationship between current stress stiffness matrix  $K_\sigma$  and actual stress inside the plate in the case of small deformation, the elastic buckling coefficient  $k$  can be easily determined by solving a typical eigenvalue equation. The elastic buckling critical stress  $\tau_{cr}$  can be written as

$$\tau_{cr} = k \frac{\pi^2 E}{12(1 - \nu^2)} \left(\frac{t}{b}\right)^2 \quad (2)$$

where  $E$  and  $\nu$  represent Young's modulus and Poisson ratio of steel, respectively.

While for the elasto-plastic buckling analysis, the situation becomes more sophisticated since the current stress stiffness matrix  $K_\sigma$  is no longer proportional to the actual stress in the plate due to the influence of geometric nonlinearity and material nonlinearity. In other words, the essence of elasto-plastic buckling analysis is the solve-seeking process of the equilibrium equations in which both geometric and material nonlinearities were considered. Hence, in order to obtain the elasto-plastic ultimate strength ( $\tau_{ult}$ ) of the perforated plate, a general-purpose finite element program should be used for the whole process analysis of the plate by gradually increasing the loads applied on the plate until the collapse occurs. In this paper, the collapse is deemed to happen at the peak point of in-plane load versus out-of-plane deflection relation curve and the elasto-plastic ultimate strength takes the greatest load during the whole loading process.

### 3.3 Finite element model

The steel used has the properties of material yield stress  $\sigma_y = 345$  MPa, shear yield stress  $\sigma_{y_s} = 199$  MPa, Young's modulus  $E = 2.06 \times 10^5$  MPa and Poisson ratio  $\nu = 0.3$ . During the elasto-plastic analysis, the steel material is assumed to be linearly elastic before yielding and perfectly plastic after yielding (i.e., with no strain hardening). The initial geometric imperfection follows the elastic buckling mode and the initial deflection amplitude is chosen to be  $b/1000$ .

Plate elements (SHELL181) with four nodes and six degrees of freedom for each node were used in the present research, with the influence of transverse shear deformation being considered (ANSYS 2009). The meshes around the circular hole and near the stiffeners are subdivided to take into account the complexity of stress distribution inside these zones. The mesh-controlling parameters for analyses are selected as follows:

1. For the unstrengthened plates (*UN*-plates), the element sizes along the plate edges and the hole edge are  $b/30$  and  $(\pi d)/120$ , respectively, indicating that the element size gradually increases by 12.5~2.5 times (for  $d/b = 0.1 \sim 0.5$ ) from the hole edge to the plate edges.
2. For the *FSA*-plates and *FSB*-plates
  - the element size along the plate edges is  $b/30$
  - the element size along the four straight intersections of plate and stiffener is  $L_b/30$
  - the element size along the plate's hole edge and the stiffener's hole edge is  $(\pi d)/120$

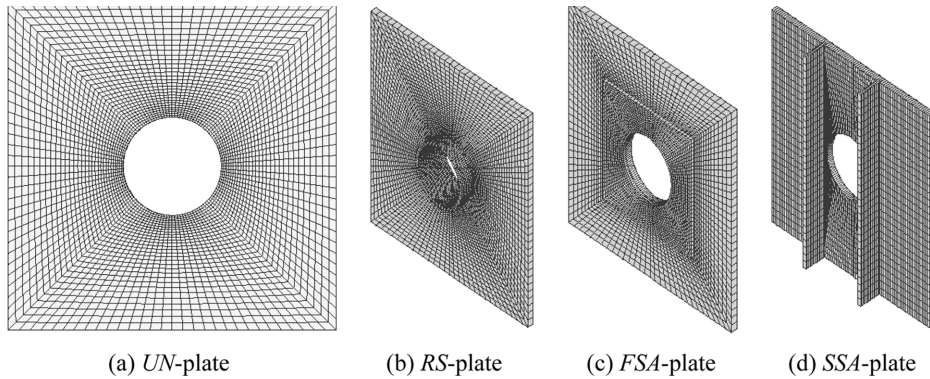


Fig. 3 Finite element meshes of the perforated plates unstrengthened or strengthened by typical stiffeners

### 3. For the *RS*-plates, *SSA*-plates, *SSB*-plates and *SSC*-plates

- the element size along the plate edges is  $b/30$
- the element size along the hole edge is  $(\pi d)/120$
- the average element size in the stiffener is  $(\pi d)/120$
- The typical finite element meshes of the studied plates produced with the previous selected mesh-controlling parameters are shown in Fig. 3. For the plates strengthened by flat stiffeners, the degrees of freedom (DOFs) of the nodes in the outer straight and inner circular edges of the flat stiffener are coupled with those of perforated plate nodes located in the same plane position to simulate the connecting effect of weld beads.

To verify the applicability of the selected mesh-controlling parameters, a mesh sensitivity study is carried out. The effect of the average element size along the plate edges on the elastic and elasto-plastic buckling stresses of the unstrengthened perforated plates with  $b/t = 30, 90$  and  $d/b = 0.3, 0.5$  are demonstrated in Fig. 4. The figure shows that the errors in  $\tau_{cr}$  and  $\tau_{ut}$  increase as the average element size is enlarged, and the maximum error for the results produced by the selected mesh-controlling parameters (i.e.,  $b/30$ ) is less than 0.7%, which is considered accurate enough for the research.

## 4. Buckling analysis results

### 4.1 Elastic buckling behavior

#### 4.1.1 Elastic buckling stress

Fig. 5 shows the variations of elastic buckling stress  $\tau_{cr}$  of the unstrengthened and strengthened perforated plates with  $b/t = 30$  and  $90$ , as plotted against  $d/b$ . It is evident from the figure that  $\tau_{cr}$  of all strengthened plates with constant hole size are decreased obviously as plate slenderness ratio is enlarged, and  $\tau_{cr}$  of all strengthened plates except for the *LSA*-plates and *LSC*-plates with  $b/t = 90$  reduce gradually with increasing hole diameter to plate width ratio when plate slenderness ratios are fixed, which is similar to the *UN*-plates. The enhancements in elastic buckling stress, when compared to the *UN*-plates, are different for the plates strengthened by various stiffeners and behave as follows:

1. For the plates strengthened by ringed stiffeners, elastic buckling stress are more or less elevated when compared to the *UN*-plates, and the increases in  $\tau_{cr}$  of the plates with small slenderness ratios (or

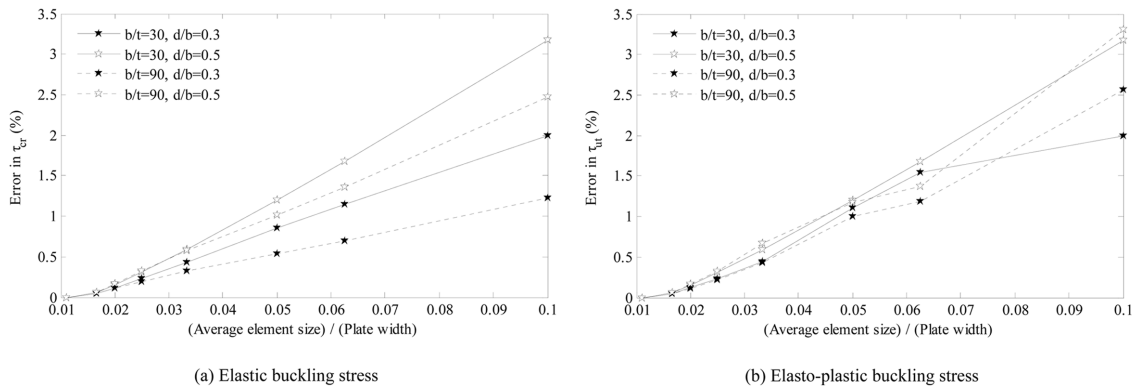


Fig. 4 Variation of error in elastic and elasto-plastic buckling stresses of UN-plates as a function of average element size along the plate edges

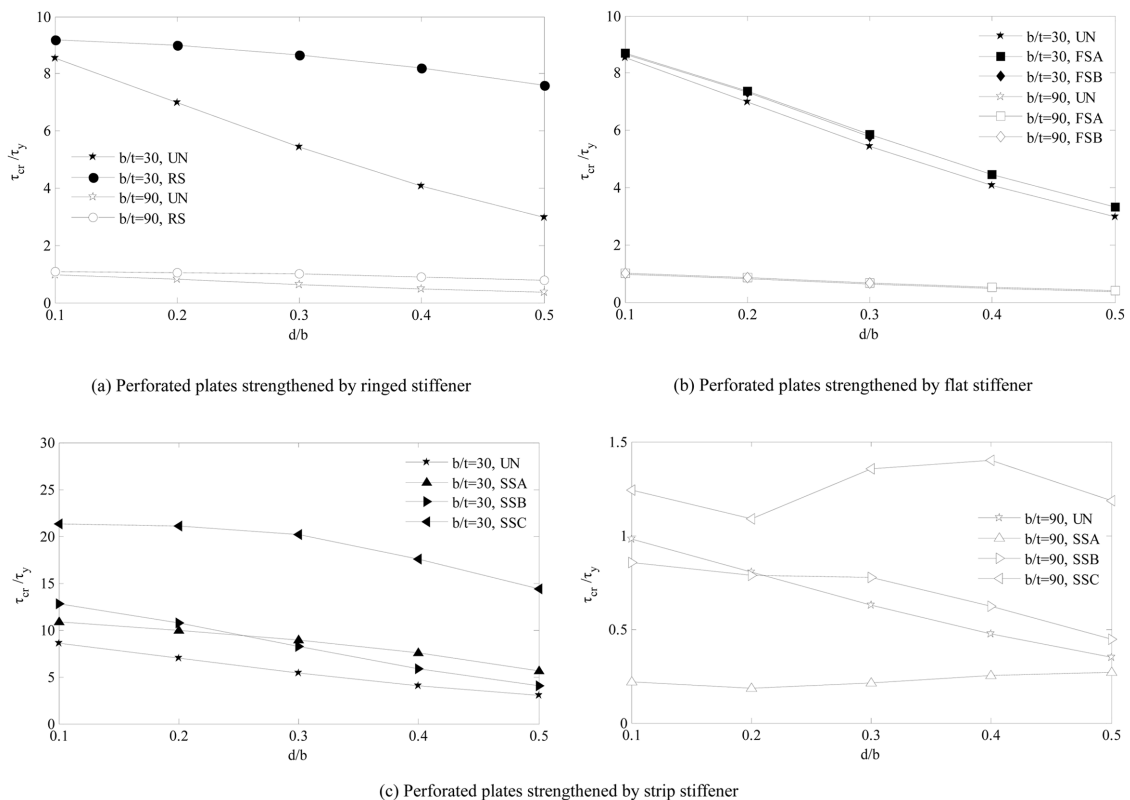


Fig. 5 Elastic buckling stresses of the unstrengthened and strengthened perforated plates under shear loading with  $b/t = 30$  and  $90$

large holes) are obviously higher than those of plates with large slenderness ratios (or small holes). Concretely,  $\tau_{cr}$  of RS-plates are  $(0.65-4.63)\tau_y$  (for  $d/b = 0.1-0.5$ ) higher than those of UN-plates for the

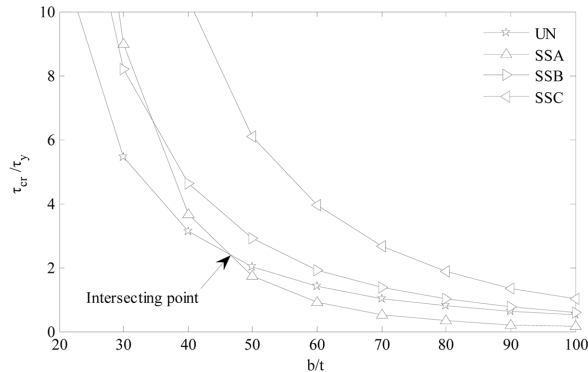


Fig. 6 Variation of elastic buckling stresses of the perforated plates strengthened by strip stiffeners as a function of plate slenderness ratio, with  $d/b = 0.3$

cases of  $b/t = 30$ , while the increases in  $\tau_{cr}$  are  $(0.09-0.45)\tau_y$  (for  $d/b = 0.1-0.5$ ) when  $b/t = 90$ .

2. For the plates strengthened by flat stiffeners, the increases in  $\tau_{cr}$  are relatively unobvious and take the values of  $(0.13-0.39)\tau_y$  and  $(0.02-0.04)\tau_y$  for the plates with  $b/t = 30$  and  $90$ , respectively. Higher increases in  $\tau_{cr}$  of the plates with smaller plate slenderness ratios are also found.

3. For the plates strengthened by strip stiffeners, the increases in  $\tau_{cr}$  of *SSC*-plates are  $(11.40-14.67)\tau_y$  for  $b/t = 30$  and  $(0.26-0.93)\tau_y$  for  $b/t = 90$ , which are obviously higher than those of *SSA*-plates and *SSB*-plates. Note that deterioration in elastic buckling behavior occurs to *SSA* since  $\tau_{cr}$  of *SSA*-plates are smaller than those of *UN*-plates. Taking a deep investigation into the variation of  $\tau_{cr}$  with  $b/t$ , as shown in Fig. 6, an intersecting point of *SSA*-curve and *UN*-curve, which is non-existent for other strip stiffeners, is observed. The elastic buckling stress of a *SSA*-plate is lower than that of *UN*-plate when  $b/t$  is larger than the value determined by the intersection point, and vice versa.

By comparison, for all cases discussed, *SSC* brings the greatest enhancement in  $\tau_{cr}$ , while *FSA* and *FSB* make the least contributions to elastic buckling behaviors of the perforated plates under shear loading. *SSA* should be avoided for the thin perforated plates with large slenderness ratios due to reductions in  $\tau_{cr}$ .

#### 4.1.2 Elastic buckling shape

Fig. 7 shows the elastic buckling shapes (i.e., out-of-plate displacement distribution patterns) of the unstrengthened and strengthened plates with  $b/t = 90$  and  $d/b = 0.3$ . It is clear that all plates considered behave one half-wave in both directions of the plate diagonal lines. Buckling bands with the largest buckling deformation being concentrated near the diagonal line connecting the two end points of edge shears, which are the features of solid or unperforated plates under shear loading, are also observed in the *UN*-plate and all strengthened plates except for *SSA*-plate. For the *SSA*-plate, a more uniformly distributed buckling deformation is found.

### 4.2 Elasto-plastic buckling behavior

#### 4.2.1 Elasto-plastic ultimate strength

Variations of elasto-plastic ultimate strength  $\tau_{ult}$  of the unstrengthened and strengthened perforated

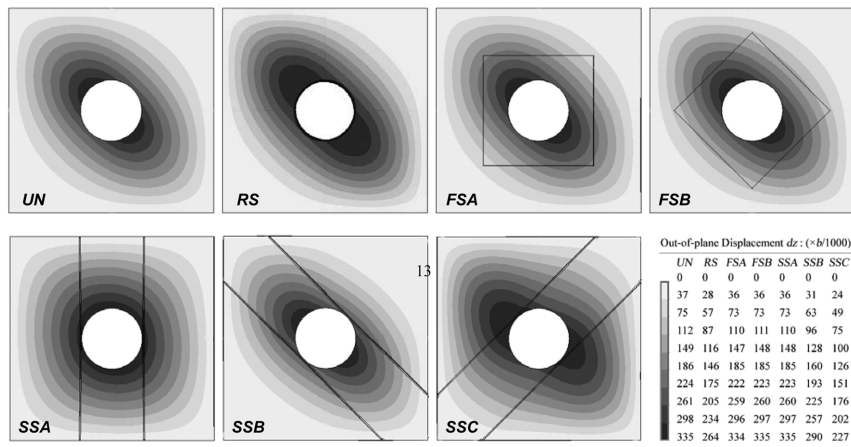
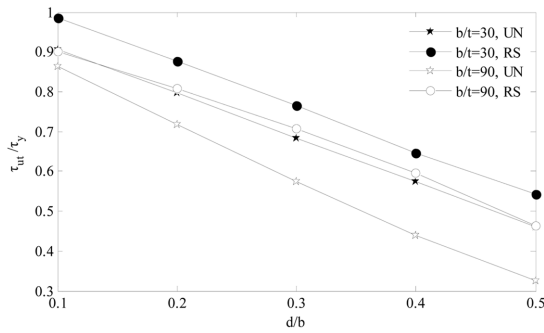
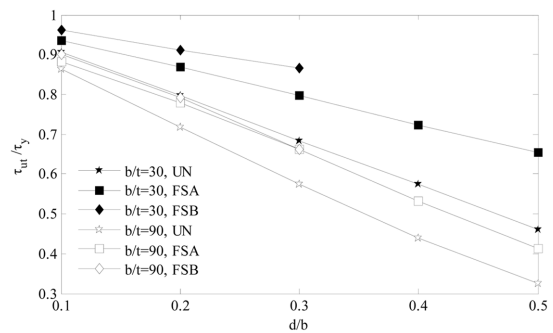


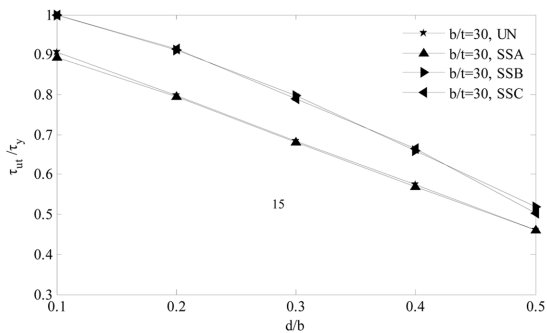
Fig. 7 Elastic buckling shapes of the unstrengthened and strengthened perforated plates under shear loading with  $b/t = 90$  and  $d/b = 0.3$



(a) Perforated plates strengthened by ringed stiffener



(b) Perforated plates strengthened by flat stiffener



(c) Perforated plates strengthened by strip stiffener

Fig. 8 Ultimate strengths of the unstrengthened and strengthened perforated plates under shear loading with  $b/t = 30$  and  $90$

plates with  $b/t = 30$  and  $90$  are demonstrated in Fig. 8, as plotted against  $d/b$ . It can be found that the

reduction in  $\tau_{ut}$  with increasing  $b/t$  or enlarging  $d/b$  is also evident. Ultimate strengths of all considered strengthened plates, except for the *SSA*-plates with  $b/t = 30$  and the *SSB*-plates with  $b/t = 90$  and  $d/b = 0.1$ , are more or less improved when compared to the *UN*-plates and the details can be described as:

1. For the plates strengthened by ringed stiffeners, the increases in  $\tau_{ut}$  of the *RS*-plates with  $b/t = 30$  and  $90$  are  $(0.072-0.084)\tau_y$  and  $(0.038-0.155)\tau_y$ , respectively, with high values occurring to the plates containing large holes.

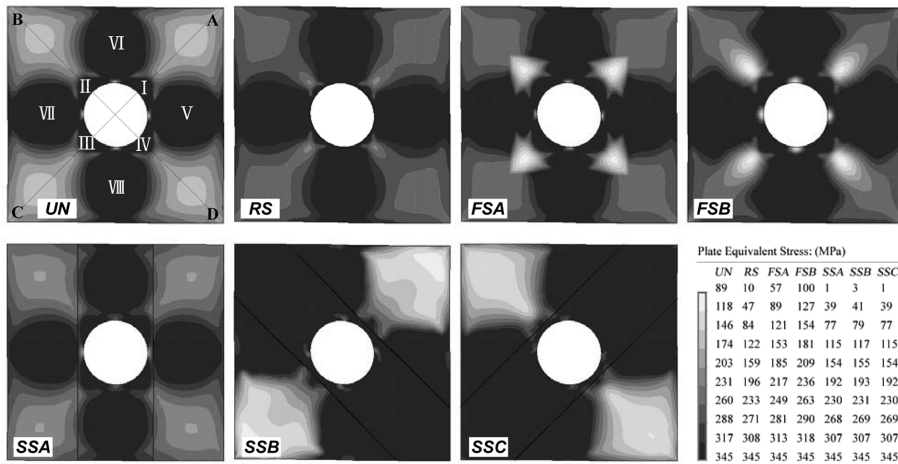
2. For the plates strengthened by flat stiffeners, the enhancements in  $\tau_{ut}$  of the strengthened plates with large holes are again more obvious than those of the plates with small holes. Take the case of  $d/b = 0.5$ ,  $\tau_{ut}$  of the *FSA*-plate with  $b/t = 30$  and  $90$  are 1.42 and 1.26 times higher than those of the *UN*-plates, respectively. Moreover, *FSB* provides higher strengthening effects than *FSA*, despite its unsuitability for the plates with very large holes (i.e.,  $d/b > 0.5$ ) due to stiffener dimensions.

3. For the plates strengthened by strip stiffeners, the situations of various  $b/t$  are different. When  $b/t = 30$ , *SSB* and *SSC* bring the highest increases (10-26%) in  $\tau_{ut}$  and that difference between the two stiffeners are negligible. However, *SSA* produces the reductions of at most 1.4% in  $\tau_{ut}$  when compared to the *UN*-plates. For the case of  $b/t = 90$ , the improvements in ultimate strength provided by *SSC* are still the maximums among all strip stiffeners, with being followed by *SSA*. Insignificant rises, even slight reduction for  $d/b = 0.1$ , in  $\tau_{ut}$  are observed for the *SSB*-plates with  $b/t = 90$ .

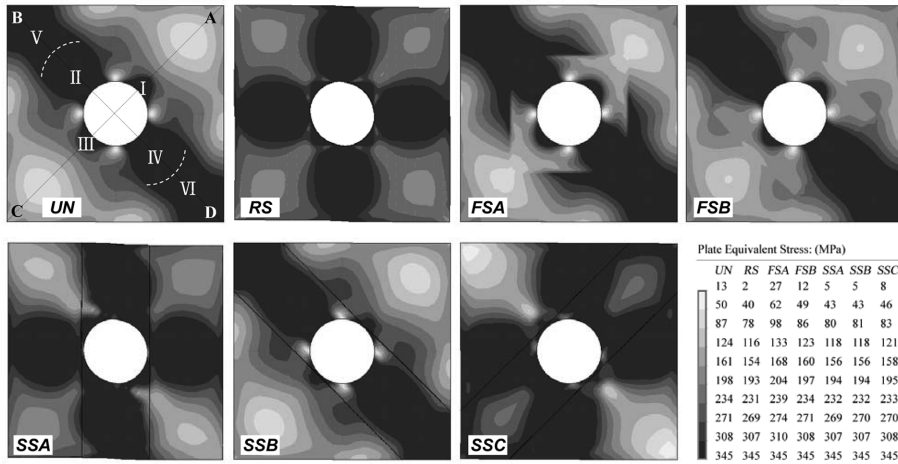
Conclusion can be made after a further comparison that *FSA* and *FSB* bring the greatest enhancements in  $\tau_{ut}$  for relatively thick plates, with *FSB* being unsuitable to the cases of very large holes, while the most effective stiffeners for relatively thin plates belong to *RS* and *SSC*. In addition, *SSA* (or *SSB*) is not suggested by the authors to be used for thick (or thin) plates due to the inconsiderable improvements even decrements in ultimate strength.

#### 4.2.2 Stress distribution in limit state

Fig. 9 shows the stress distributions in limit state of the unstrengthened and strengthened perforated plates with  $b/t = 30$  and  $d/b = 0.3$ . The black areas represent the plastic zones where the equivalent stresses are the highest and equal to yield stress. It is evident that, for the *UN*-plate with  $b/t = 30$ , the plastic zones are composed of eight subzones, i.e., four zones of I-IV near the hole edge and four zones of V-VIII adjacent to the midpoints of the plate edges. Among them, zones I and III are dominated by the principal tensile stresses parallel to line BD (i.e., the diagonal line connecting the two end points of edge shears), while zones II and IV are dominated by the principal compressive stresses parallel to line AC (i.e., the diagonal line connecting the two start points of edge shears). As for the plastic zones V-VIII, the plate yielding occurs mainly due to the shear stresses. For the *RS*-plate, *FSA*-plate and *FSB*-plate with  $b/t = 30$ , there are little changes in the stress distributions when compared to the *UN*-plate with  $b/t = 30$ , and  $\tau_{ut}$  of these strengthened plates are enhanced primarily due to the increases in the area of high stress zones including plastic zones. The considerable contribution to the shear bearing area provided by the flat stiffeners should not be ignored and may be a plausible explanation for the higher  $\tau_{ut}$  of *FSA*-plate and *FSB*-plate than that of *RS*-plate. *SSA* does almost no influence on the limit state (including stress distribution and ultimate strength) of the perforated plate with  $b/t = 30$ . While for the plates strengthened by other strip stiffeners, the plastic zones induced by the principal compressive stresses (i.e., zones II and IV of the *UN*-plate) for the *SSB*-plate and by the principal tensile stresses (i.e., zones I and III of the *UN*-plate) for the *SSC*-plate are significantly enlarged and some new plastic zones inside the plate and near the stiffener ends emerged. The expansion of plastic zones, as the results of further development of material plasticity, is the root cause of increases in  $\tau_{xu}$  of *SSB*-plate and *SSC*-plate with  $b/t = 30$ .



(a) Plates with  $b/t=30$  and  $d/b=0.3$



(b) Plates with  $b/t=90$  and  $d/b=0.3$

Fig. 9 Von Mises stress distributions in limit state of the unstrengthened and strengthened perforated plates under shear loading

For the situations of  $b/t = 90$ , the shear stress induced plastic zones adjacent to the midpoints of four edges of the *UN*-plate disappear, and a consecutive yield band along line *BD*, in which zones *II* and *IV* yield due to the principal compressive stresses parallel to line *AC* and zones *V* and *VI* yield due to the shear stresses, comes into being. *SSB* does little alteration in stress distribution and  $\tau_{ult}$  of *SSB*-plate is enhanced by a very low percentage of 3.8% when compared to the *UN*-plate. The ultimate strengths of the *FSA*-plate and *FSB*-plate with  $b/t = 90$  are improved due to the contribution of flat stiffener to shear bearing area, despite that the similar yield band has also been observed in the plate. As for the *RS*-plate and *SSA*-plate with  $b/t = 90$ , four zones adjacent to the midpoints of the plate edges, which are the features of the plates with  $b/t = 30$ , are observed for each plate, and the ultimate strengths of these strengthened plates are greatly improved because the plate materials are more fully utilized when compared to the *UN*-plate with  $b/t = 90$ . The differences in stress distributions of the *SSC*-plates with  $b/t = 90$  and  $b/t = 30$  are also observed.

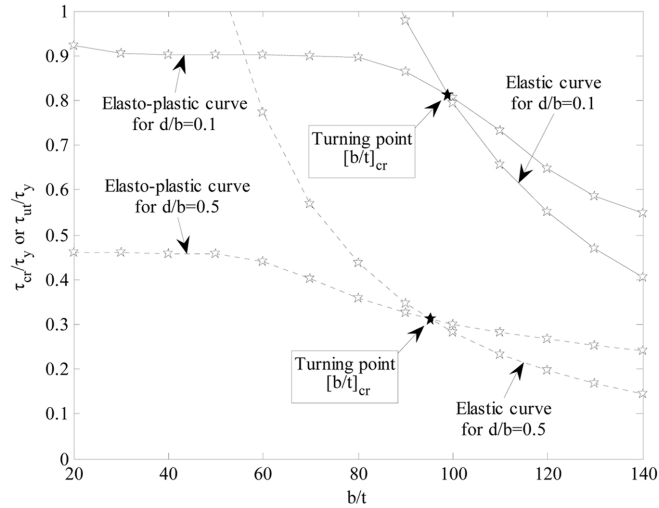


Fig. 10 Elastic and elasto-plastic buckling stresses of unstrengthened perforated square plates under shear loading with centric circular holes

$t = 30$  and  $90$  are relatively insignificant. Taken together, for the cases of large slenderness ratios, the strengthened perforated plates containing several separate yield zones adjacent to the midpoints of the plate edges in the limit state behave higher shear bearing capacities than those with a narrow and consecutive yield band along the diagonal line connecting the two end points of edge shears.

#### 4.3 Elastic buckling versus elasto-plastic buckling

It has been reported by Pellegrino *et al.* (2009) that there exists a critical slenderness ratio  $[b/t]_{cr}$  by which the practical buckling/failure pattern (i.e., elastic or elasto-plastic buckling) of an unstrengthened perforated plate under shear loading is determined. Fig. 10 demonstrates the elastic and elasto-plastic buckling stresses of unstrengthened perforated square plates under shear loading with centric circular holes, as plotted against  $b/t$ . It is clear that  $\tau_{cr}$  is normally larger than  $\tau_{ut}$  even  $\tau_y$  (i.e., plate fails due to elasto-plastic buckling rather than elastic buckling) for a thick plate with  $b/t < [b/t]_{cr}$ , and the situation is reversed (i.e., elastic buckling occurs first and  $\tau_{ut}$  is higher than  $\tau_{cr}$  due to the post-buckling behavior) for the cases of  $b/t > [b/t]_{cr}$ . Moreover, the difference between  $\tau_{cr}$  and  $\tau_{xu}$ , i.e., the so-called post-buckling strength of the thin plates with  $b/t > [b/t]_{cr}$ , enlarges gradually as  $b/t$  is increased.

A similar situation appears in the strengthened perforated plates and the critical slenderness ratios of shear loaded unstrengthened and strengthened perforated plates with varying hole diameter to plate width ratios are shown in Fig. 11. It can be seen from the figure that  $[b/t]_{cr}$  of SSA-plates are restricted to a narrow value range of 62~77 which is much lower than other plates. RS-plates and SSC-plates have the highest  $[b/t]_{cr}$  which are larger than 98, with  $[b/t]_{cr}$  being significantly increased as  $d/b$  is enlarged. This is mainly because that the increases in  $\tau_{cr}$  of RS-plates and SSC-plates are especially larger than the  $\tau_{ut}$  enhancements (i.e., the elastic curves in Fig. 10 have been more greatly shifted up than the elasto-plastic curves). As for the FSA-plates and FSB-plates,  $[b/t]_{cr}$  decrease slightly with increasing  $d/b$ , which is similar to the UN-plates, while  $[b/t]_{cr}$  of these two types of strengthened plates are decreased by at most 11% and 7%, respectively, when compared to the unstrengthened ones.

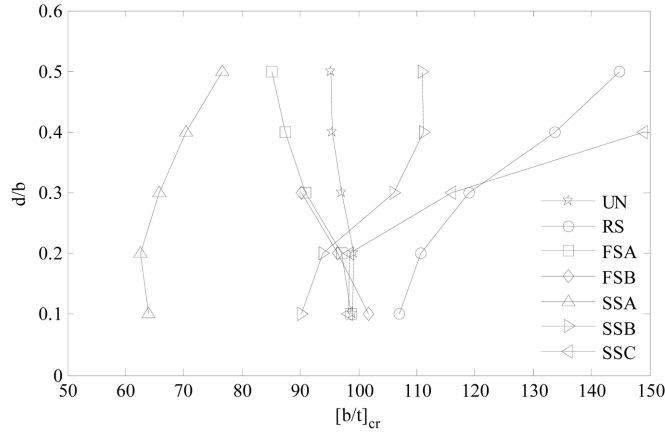


Fig. 11 Critical slenderness ratios of the unstrengthened and strengthened perforated plates under shear loading

## 5. Comparison of strengthening efficiency

The previous analyses are undertaken on the basis of the selected geometric sizes of stiffeners as introduced earlier, implying that buckling behavior improving of strengthened plates are obtained at various costs of stiffener consumption which has been the concern of designers. In this regard, further comparisons of strengthening efficiency are carried out by defining the increases in  $\tau_{cr}$  and  $\tau_{ut}$  produced by unit weight of stiffener as strengthening efficiency indexes (i.e.,  $\delta\tau_{cr}$  and  $\delta\tau_{ut}$ ) which can be expressed as follows

$$\delta\tau_{cr} = \frac{(\tau_{cr} \text{ of strengthened plate} - \tau_{cr} \text{ of unstrengthened plate})}{\tau_y W_{\text{stiffener}}} \quad \text{for elastic buckling}$$

$$\delta\tau_{ut} = \frac{(\tau_{ut} \text{ of strengthened plate} - \tau_{ut} \text{ of unstrengthened plate})}{\tau_y W_{\text{stiffener}}} \quad \text{for elasto-plastic buckling}$$

where  $W_{\text{stiffener}}$  represents the stiffener weight per unit weight of the plate (with hole related weight being neglected) and can be calculated as

$$W_{\text{stiffener}} = \frac{\pi d h_a t_a}{b^2 t} \quad \text{for RS}$$

$$W_{\text{stiffener}} = \frac{L_b^2 t_b}{b^2 t} \quad \text{for FSA and FSB}$$

$$W_{\text{stiffener}} = \frac{2 b h_c t_c}{b^2 t} \quad \text{for SSA}$$

$$W_{\text{stiffener}} = \frac{2(\sqrt{2}b - d - 3t)h_c t_c}{b^2 t} \quad \text{for SSB and SSC}$$

Table 1 Strengthening efficiency indexes of the strengthened perforated plates under shear loading

		Elastic buckling ( $\delta\tau_{cr}$ )						Elasto-plastic buckling ( $\delta\tau_{ul}$ )					
		RS	FSA	FSB	SSA	SSB	SSC	RS	FSA	FSB	SSA	SSB	SSC
$b/t=30$	$d/b=0.1$	24.7	10.6	8.2	17.5	25.4	75.8	3.0	1.8	3.4	-0.1	0.6	0.6
	$d/b=0.3$	40.9	2.7	2.3	26.4	19.3	103.4	1.0	0.8	1.2	0.0	0.8	0.8
	$d/b=0.5$	35.3	0.8	N/A	19.8	8.7	98.9	0.6	0.5	N/A	0.0	0.5	0.4
$b/t=60$	$d/b=0.1$	14.1	2.7	2.2	-17.1	4.5	20.2	3.2	2.2	3.6	-0.7	0.7	0.8
	$d/b=0.3$	21.0	0.7	0.6	-7.4	7.2	35.2	1.1	0.7	1.2	0.0	0.5	1.1
	$d/b=0.5$	17.1	0.2	N/A	2.1	4.4	38.5	1.2	0.4	N/A	0.3	0.2	0.9
$b/t=90$	$d/b=0.1$	9.8	1.2	1.1	-17.1	-2.2	4.5	4.3	1.3	2.3	0.8	-0.2	1.3
	$d/b=0.3$	13.8	0.3	0.3	-9.3	3.0	14.9	5.1	0.6	0.6	2.4	0.4	3.1
	$d/b=0.5$	10.3	0.1	N/A	-1.7	2.5	21.0	3.1	0.2	N/A	2.1	0.3	3.4

Table 1 lists the strengthening efficiency indexes of the strengthened perforated plates under shear loading. Results reveal that *SSC* behaves the highest strengthening efficiency for improving the elastic behaviors of all perforated plates under shear loading except the plates with  $b/t = 90$  and  $d/b = 0.1$ . As for the cases of elasto-plastic buckling, *RS* can provide high enhancements in  $\tau_{ul}$  at low costs of stiffener consumption for all discussed perforated plates, and there exists a better choice of *FSB* for the plates with small slenderness ratios (e.g.,  $b/t \leq 60$ ) and small hole diameters (e.g.,  $d/b \leq 0.3$ ) or of *SSC* for the plates with large slenderness ratios (e.g.,  $b/t \geq 60$ ) and large hole diameters (e.g.,  $b/t \geq 0.5$ ). Despite the inaccuracy caused by the nonlinearity between buckling stress improvement and stiffener consumption for the same type of strengthened perforated plates, the previous conclusions may be useful for selecting the most effective and economical strengthening stiffener for shear loaded perforated plates in practical engineering.

## 6. Conclusions

The present study is dedicated to the buckling behaviors of shear loaded perforated steel plates strengthened by three types of stiffeners, i.e., ringed stiffener, flat stiffener and strip stiffener. A series of ANSYS elastic and elasto-plastic buckling finite element analyses are carried out with various plate slenderness ratios as well as circular hole diameter to plate width ratios.

The results show that the buckling behaviors of strengthened perforated plates are similar with those of unstrengthened ones. Reductions in  $\tau_{cr}$  of *SSB*-plates with  $b/t = 90$  and  $d/b = 0.1$  and in  $\tau_{ul}$  of *SSA*-plates with  $b/t = 30$ , when compared to the *UN*-plates, are observed, while the elastic buckling stresses and elasto-plastic ultimate strengths of other strengthened perforated plates are more or less improved due to the presence of stiffeners. The increase amplitudes in buckling strength are greatly influenced by the factors including stiffener type, plate slenderness ratio and hole diameter to plate width ratio etc. By comparison, *SSC* gives the best strengthening effects in elastic buckling stress for all perforated plates when stiffeners take the commonly used geometric sizes as mainly discussed in this paper, while the greatest increases in elasto-plastic ultimate strengths for relatively thick (or thin) perforated plates are obtained from *FSA* and *FSB* (or *RS* and *SSC*). The critical slenderness ratios of *RS*-plates and *SSC*-plates (or *SSA*-plates) are obviously higher (or lower) than those of *UN*-plates, indicating that the elasto-plastic buckling (or elastic buckling) is more likely to occur for these strengthened plates when compared

to unstrengthened ones. Contrastive analyses considering the influence of stiffener consumption reveal that *SSC* (or *RS* and *FSB*) provide the highest strengthening efficiency for improving the elastic (or elasto-plastic) behaviors for shear loaded perforated square plates containing centrally placed circular holes.

The achievements will be useful for the cutout-strengthening method selection of perforated plates and for the buckling behavior prediction of strengthened perforated plates in practical engineering.

## Acknowledgement

The present research was undertaken with support from the National Natural Science Foundation of China (no.51008193) and from the Specialized Research Fund for the Doctoral Program of Higher Education Funded by the Ministry of Education of P.R.C. (no.20090073120012).

## References

- ANSYS. (2009), Software package, Version 12.0.1.
- Azizian, Z.G. and Roberts, T.M. (1983), "Buckling and elasto-plastic collapse of perforated plates", *Proceedings of the International Conference on Instability and Plastic Collapse of Steel Structures*, London, August.
- Brown, C.J. (1990), "Elastic buckling of perforated plates subjected to concentrated loads", *Comp. and Struct.*, **36**(6), 1103-1109.
- Brown, C.J. and Yettram, A.L. (1986), "The elastic stability of square perforated plates under combination of bending, shear and direct load", *Thin-Walled Struct.*, **4**(3), 239-246.
- Brown, C.J., Yettram, A.L. and Burnett, M. (1987), "Stability of plates with rectangular holes", *J. of Struct. Eng.*, **113**(5), 1111-1116.
- Cheng, B. and Zhao, J. (2010), "Strengthening of perforated plates under uniaxial compression: Buckling analysis", *Thin-Walled Struct.*, **48**(12), 905-914.
- El-Sawy, K.M. and Nazmy, A.S. (2001), "Effect of aspect ratio on the elastic buckling of uniaxially loaded plates with eccentric holes", *Thin-Walled Struct.*, **39**(12), 983-998.
- El-Sawy, K.M., Nazmy, A.S. and Martini, M.I. (2004), "Elasto-plastic buckling of perforated plates under uniaxial compression", *Thin-Walled Struct.*, **42**(8), 1083-1101.
- El-Sawy, K.M. and Martini, M.I. (2007), "Elastic stability of bi-axially loaded rectangular plates with a single circular hole", *Thin-Walled Struct.*, **45**(1), 122-133.
- El-Sawy, K.M. and Martini, M.I. (2010), "Stability of biaxially loaded square plates with single central holes", *Ships and Offshore Structures*, **5**(4), 283-293.
- Komur, M.A. (2011), "Elasto-plastic buckling analysis for perforated steel plates subject to uniform compression", *Mech. Res. Comm.*, **38**(2), 117-122.
- Maiorana, E., Pellegrino, C. and Modena, C. (2011), "Elasto-plastic behaviour of perforated steel plates subjected to compression and bending", *Steel and Comp. Struct.*, **11**(2), 131-147.
- Moen, C.D. and Schafer, B.W. (2009), "Elastic buckling of thin plates with holes in compression or bending", *Thin-Walled Struct.*, **47**(12), 1597-1607.
- Narayanan, R. and Chow, F.Y. (1984), "Ultimate capacity of uniaxially compressed perforated plates", *Thin-Walled Struct.*, **2**(3), 241-264.
- Narayanan, R. and Rockey, K.C. (1981), "Ultimate load capacity of plate girders with webs containing circular cut-outs", *Proceedings of the Institution of Civil Engineers*, London, March.
- Paik, J.K. (2007), "Ultimate strength of perforated steel plates with a single circular hole under axial compressive loading along short edges", *Ships and Offshore Struct.*, **2**(4), 355-360.
- Paik, J.K. (2007), "Ultimate strength of perforated steel plates under edge shear loading", *Thin-Walled Struct.*

- 45(3), 301-306.
- Paik, J.K. (2008), "Ultimate strength of perforated steel plates under combined biaxial compression and edge shear loads", *Thin-Walled Struct.*, **46**(2), 207-213.
- Pellegrino, C., Maiorana, E. and Modena, C. (2009), "Linear and non-linear behaviour of steel plates with circular and rectangular holes under shear loading", *Thin-Walled Struct.*, **47**(6-7), 607-616.
- Sabir, A.B. and Chow, F.Y. (1983), "Elastic buckling of flat panels containing circular and square holes", *Proceedings of the international conference on instability and plastic collapse of steel structures*, London, August.
- Shanmugam, N.E. and Narayanan, R. (1982), "Elastic buckling of perforated square plates for various loading and edge conditions", *Proceedings of the international conference on finite element methods*, Shanghai, August.
- Shanmugam, N.E., Thevendran, V. and Tan, Y.H. (1999), "Design formula for axially compressed perforated plates", *Thin-Walled Struct.*, **34**(1), 1-20.
- Wang, G., Sun, H., Peng, H. and Uemori, R. (2009), "Buckling and ultimate strength of plates with openings", *Ships and Offshore Structures*, **4**(1), 45-53.

CC